Light Metals 2014
Edited by: John Grandfield
TMS (The Minerals, Metals & Materials Society), 2014

THE STRUCTURE, PHASE COMPOSITION AND MECHANICAL PROPERTIES OF HOT PRESSED METAL MATRIX NANOCOMPOSITES Al-Al_4C_3

S. Vorozhtsov[1,2], A. Vorozhtsov[1,3], S. Kulkov[1,2]

[1]National research Tomsk state university, Lenin str., 36, Tomsk, 634050, Russia
[2]Institute of Strength Physics and Materials Science of the SB RAS, Akademichesky str. 2/4, Tomsk, 634021, Russia
[3]Institute for Problems of Chemical and Energetic Technologies of the SB RAS, Socialisticheskaya, 1
Biisk, 659322, Russia

Keywords: Composite material, Hot pressing, Aluminum, Carbon, Aluminum carbide, Strength.

Abstract

It was shown that hot pressing of powder mixtures Al-C (n-diamond) leads to the formation of aluminum carbide Al_4C_3 in the metal matrix; the intensity of the phase Al_4C_3 formation is greater the higher the carbon content in the initial mixture. According to the X-ray analysis the compound $Al_4C_3$was finely structure with an average crystal size for the metal matrix was 40 nm and for aluminum carbide - 30 nm. Was found that increasing the volume fraction of the phase Al_4C_3 in the aluminum matrix leads to increased mechanical characteristics of the composite. For samples with 5% C in initial mixture, the ultimate strength was 400 MPa, whereas for 10% C and a half times higher - 600 MPa. Furthermore, increases as the total inelastic deformation to failure from 3 to 5% and the effective elastic modulus (E_{ef}).

Introduction

At present time Al and Al based alloys are widely used materials and the problem of improvement of their mechanical properties is particularly topical. It is known [1,2], that embedding of high-modulus nanocrystalline particles into Al matrix provides significant improvement of its mechanical properties (Young's modulus, strength, hardness), durability, thermal stability etc. [3]. At present Al-matrix composites are of specific interest for researchers due to high strength properties, operational performance, corrosion resistance and light weight. The methods of powder metallurgy are widely used for production of these materials. The method of hot pressing [4] is of particular interest. Aluminum oxide, aluminum nitride, silicon carbide and others are usually used as reinforcing particles in such composites. Embedding of carbon in the form of nanodiamonds (further n-diamond) into the soft metal matrix is considered as a relevant method. Detonation n-diamonds can affect physical and mechanical properties of composites [4,5]. In the process of hot pressing ultrafine aluminum carbide (Al_4C_3) particles reinforcing the matrix [5] are formed in Al-C composite as it is shown in [4,5]. However, the properties of such materials have not been studied.
The objective of this work is to study the formation of structure, phase composition and mechanical properties of metal-matrix composites Al–Al_4C_3 in the process of hot pressing.

Experimental

The materials for investigations were nanocrystalline aluminum powders, synthesized by electrical explosions of conductors [6] in argon atmosphere, followed by exposure to air, at which the partly oxidation of the metal, in this case hydrogen not formed; and n-diamond, synthesized by detonation method [7,8]. The average size of individual particles and agglomerates in powders, and that of dispersed inclusions in the structure of the materials, were determined by means of random secants [9].
The phase composition and structural parameters of the initial powders and the materials based on them was studied on diffractometer using Cu$K\alpha$ radiation. Recording was performed by points with steps of 0.02–0.1 deg in the range of 20 deg < 2θ < 120 deg with an exposure duration of 10 s. The phases were identified by comparing the peaks of the X-ray diffraction pattern with the ASTM Data File. The crystallite sizes (or sizes of coherently diffracting domains (CDD)) were determined from X-ray peaks by broadening the most intense reflection at narrow angles of diffraction, while the microdistortion of the crystal lattice (ε) was calculated by broadening reflections at wide angles of diffraction [10].
The materials were obtained with various n-diamonds contents (from 1 to 30 wt %) from the investigated powders through hot pressing in argon at a temperature of 873 K and a pressure of 30 MPa. The isothermal pressing time was 40 min. After hot pressing, the total pore volume for the samples containing 10% n-diamond was about 20%, while for materials with 30% n-diamonds - 45%.
The structure of these materials was studied by means of optical metallography on a Neophot 21 microscope and scanning electron microscopy (SEM) on a SEM 515 (Philips).
Mechanical tests were conducted in an Instron 1185 universal testing machine. The microhardness of the materials was measured using a Nano Indenter G200/XP with a load of 250 g.

Results and discussion

Figure 1 shows the SEM images of the aluminum powder and the size distribution of the agglomerates and particles in it, Figure 2. It was established that the average agglomerate size in the powder was 14 μm, while the size of the particles in them was 700 nm. According to the data from X-ray analysis, the average crystallite size in the aluminum powder was 90 nm, and the microdistortion of the crystal lattice was 10^{-3}.
Figure 3 shows SEM images of the n-diamond powder and the size distribution for the agglomerates on the Figure 4. Their average size was 11 μm, while that of their constituting microblocks [11] (according to data from low angle X-ray scattering) was 4 nm. According to the results from X-ray phase analysis, the nanocrystalline carbon (40±5%) and a diamond phase (45±5%), with traces of a crystalline carbon phase. According to the X-ray data, the average crystallite size in the n-diamond powder was 4 nm, and the microdistortion of the crystal

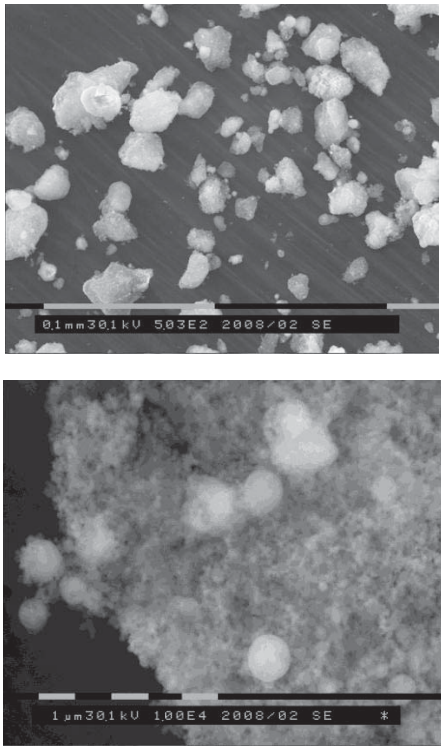

Figure 1. SEM images of the aluminum powder

lattice was 17×10^{-3}; i.e., carbon was present in single domain particles.

Figure 5 shows the SEM image of a surface of hot pressed material. It can be seen that it is porous, and the pores are distributed nonuniformly in the material. Poreless light and gray segments are distinguishable in its structure.

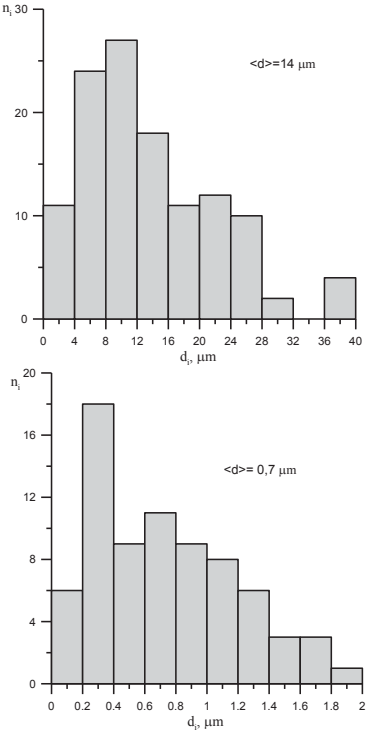

Figure 2. Size distribution of agglomerates (top) and particles (bottom)

Since the average size of the light segments (Fig.6) on the material's surface is comparable to the average agglomerate size in the aluminum powder, this provides grounds for believing that they are sintered aluminum agglomerates that entered into the reaction with carbon less than the finer particles in immediate contact with the carbon. This conclusion was confirmed by the measured microhardness of the material being 1050 MPa for the light segments and 1780 MPa for the darker ones (the value of the hardness for the matrix aluminum without reinforcing nanoparticles is 750 MPa).

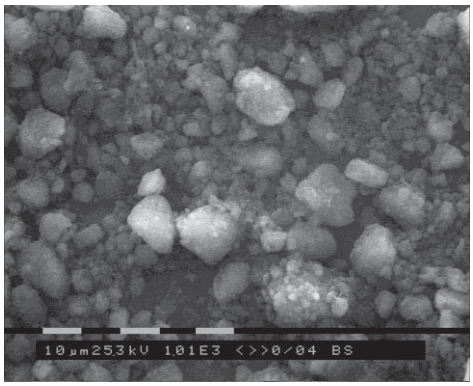

Figure 3. SEM image of the n-diamond powder

Determination of the average pore size (Fig. 7) showed they were comparable to the agglomerates in the n-diamond powder. This demonstrates that the materials became porous during the burning out of carbon (mainly of its amorphous component) that did not join in the reaction during the hot pressing of the powder mixture.

Thus, the studies of macrostructure have found porosity, which is probably related to burning out of amorphous carbon. Therefore the light and gray areas have different content of nanoparticles. A more detailed study of the microstructure will be devoted to further research.

The X-ray diffraction patterns of the synthesized samples (Fig. 8) contain reflections of aluminum and the aluminum carbide Al_4C_3 [4,5,12] that was formed during hot pressing.

The average crystallite size in the materials due to the broadening of the X-ray reflections was 40 nm for the metal matrix and 30 nm for aluminum carbide.

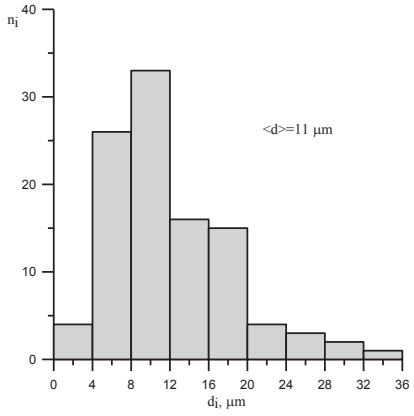

Figure 4. Size distribution of agglomerates in n-diamond powder

The evaluation of the average size of aluminum crystallites thus showed that it was 40 nm, i.e., larger than the one found from the mixture rule.

This is because the X-ray diffraction pattern, which is an integral characteristic of the material, determines the broadening of X-ray reflections both for the aluminum crystallites that joined in the chemical reaction with the carbon and the crystallites of that part of the metal matrix barely reacted (if at all).

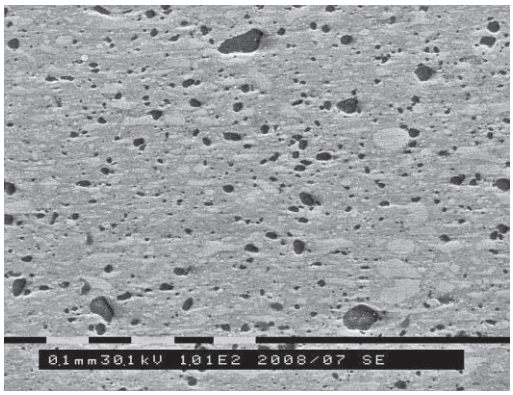

Figure 5. SEM image of the surface of the hot pressed material

As a consequence, the calculated sizes of coherently diffracting domains are larger than might be expected. Another reason for the variation in crystallite size inside the aluminum matrix could be the emergence of thermal stresses upon the relatively rapid (~150°C/min) cooling of the material from the synthesis temperature.

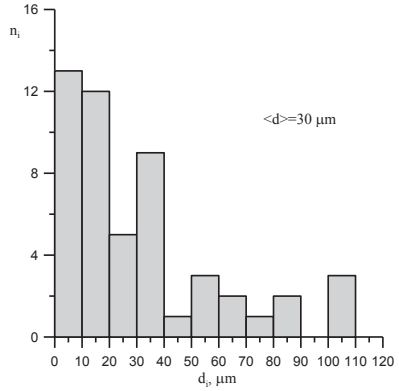

Figure 6. Size distribution of the light areas in the hot pressed material

The calculated lattice parameters for aluminum and its carbide differ negligibly from the tabulated values [13]. They are a = 0.33618 nm and c = 2.3689 nm for Al_4C_3 and a = 0.40516 nm for aluminum. Microdistortions of the crystal lattice are 2×10^{-3} for aluminum and 9×10^{-3} for Al_4C_3.

Figure 9 shows the dependence of the ratio of sum of intensities for Al_4C_3 (012) and Al (111) versus of the amount of n-diamond introduced into the initial nanopowder mixture. It can be seen that as the carbon content rises, the amount of Al_4C_3 phase grows substantially.

Figure 10 illustrates the dependence of variations in the crystallite size for the metal matrix and aluminum carbide on the relative content of aluminum carbide, normalized for aluminum content. It was established that as the amount of formed Al_4C_3 rose during the material's synthesis, the crystallite size of the metal matrix diminished while that of the crystallites of the Al_4C_3 phase grew.

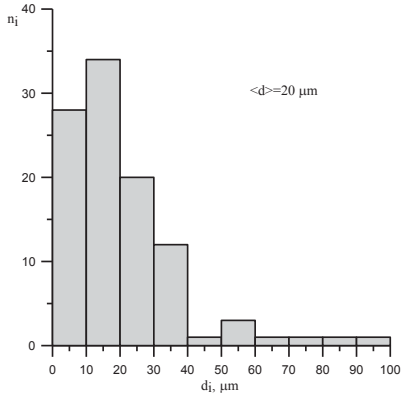

Figure 7. Size distribution of the pores in the hot pressed material

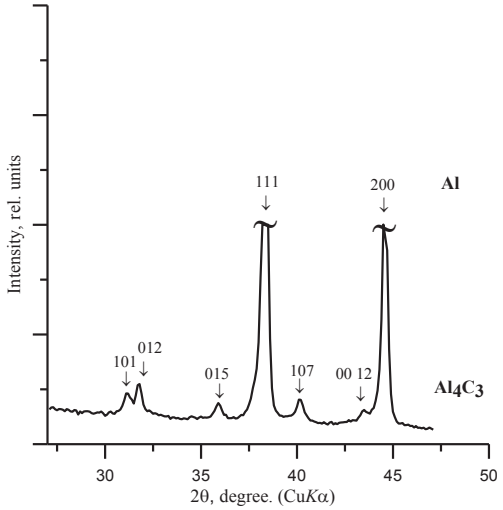

Figure 8. Fragment of the X-ray diffraction pattern of Al–Al_4C_3 material obtained by hot pressing.

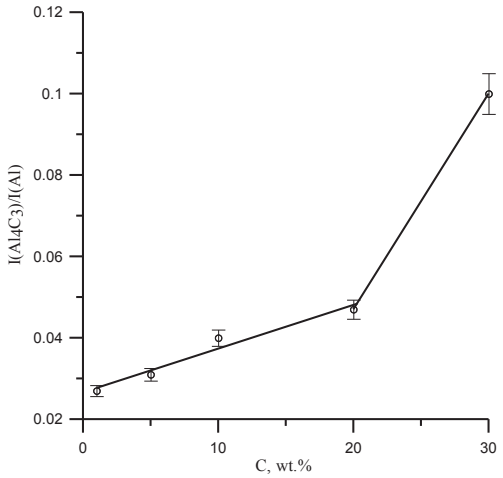

Figure 9. Dependence of the ratio of integral intensities of the Al_4C_3 (012) and Al (111) reflections on the n-diamond content in the powder mixture.

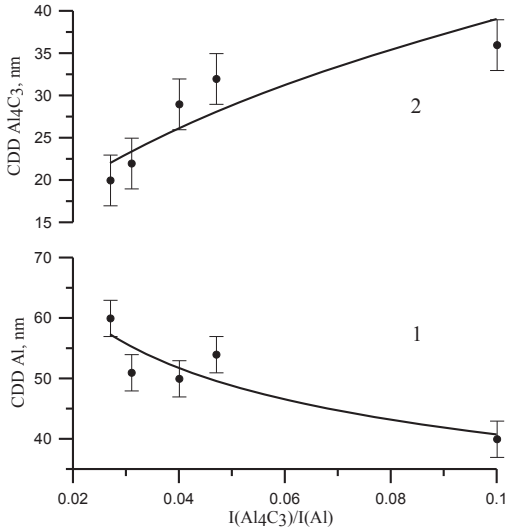

Figure 10. Dependence of the crystallite size for (1) the metal matrix and (2) aluminum carbide depending on the ratios of the integrated intensities of Al_4C_3 (012) and Al (111) reflections

Figure 11 shows loading diagrams of hot-pressed Al–Al_4C_3 composites with 5 and 10 wt.% C added to the initial powder mixture. As the volume fraction of carbon in the initial mixture and hence of aluminum carbide in the composites produced is increased, the mechanical characteristics of the materials are seen to change dramatically (Table I). For specimens with 5 wt.% C in the initial mixture, the yield stress $\sigma_{0.2}$ was 190 MPa, whereas for 10 wt.%C, $\sigma_{0.2}$ was as high as 300 MPa, whereas for the aluminum matrix material without reinforcing particles $\sigma_{0.2}$ was 170 MPa. The total inelastic fracture strain increased from 3 to 5%, whereas the effective elastic modulus E_{ef} found from the stress-strain curves was 20 GPa for the material without reinforcement nanoparticles, 21 GPa for 5 wt.% C and 29 GPa for 10 wt.% C.

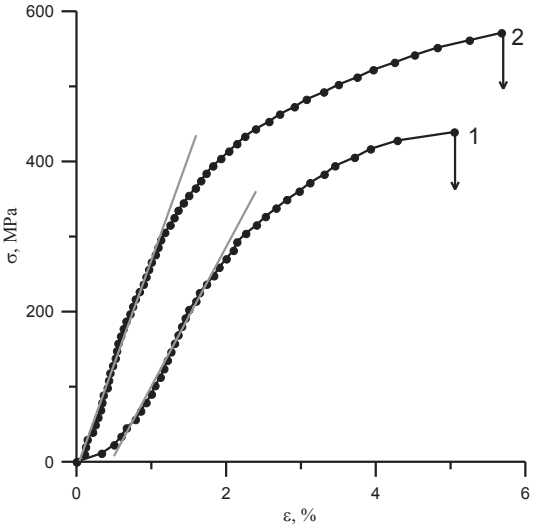

Figure 11. Loading diagrams of Al–Al_4C_3 composites: Al - 5 wt.% C (1) and Al - 10 wt.% C (2).

The data on the size of coherently diffracting domains and microstrains as a function of macrostresses were obtained under step loading, with the X-ray patterns being taken for each loading step. Figure 12 shows dependence of the size of the coherently diffracting domains in the aluminum matrix from the applied macrostresses. The plots exhibit two stages: (1) the size of the coherently diffracting domains remains fixed up to a limiting value of the macrostresses and (2) the crystallite size reduces drastically at a higher

Table I. The Mechanical Properties of Al–Al_4C_3 Composites

Carbon content in initial mixture, wt. %	Yield stress, $\sigma_{0.2}$, MPa	Effective elastic modulus, E_{ef}, GPa	Total inelastic fracture strain, $\Delta\varepsilon$, %
0	170	20	2.5
5	190	21	3
10	300	29	5

macrostress level. Apparently, the obtained values of 65 and 100 MPa for the compositions studied are defined yield strength of the matrix at the microscale. What is more, an increase in the carbon content in the initial mixture causes the amount of the reinforcement to increase and the matrix crystallite size to decrease. The Al_4C_3 CDD size varies but little with applied loading (from 20 to 16 nm), as seen in Fig. 13.

We have calculated the microstresses at work in the matrix from aluminum reflection broadening at high diffraction angles, as the applied macrostresses are varied (Fig. 14).

The microstresses are seen to be linearly dependent on the applied macrostresses, whereas the inflection of curve 2 for σ = 200 MPa is attributable to the attainment of the yield stress in the matrix. Thus, the results obtained are evidence of the fact that an increase in the volume fraction of Al_4C_3 in the aluminum matrix causes the mechanical characteristics of the composites to increase.

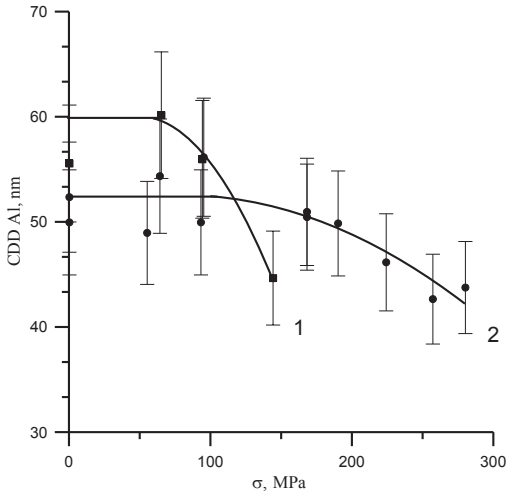

Figure 12. Variations of coherently diffracting domains (CDDs) in aluminum with applied stress under step loading. 1-Al-5%C; 2-Al-10%C.

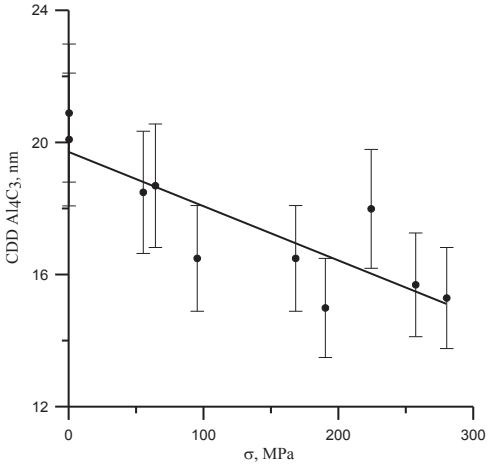

Figure 13. Variations of the CDD size in Al_4C_3 with applied loading.

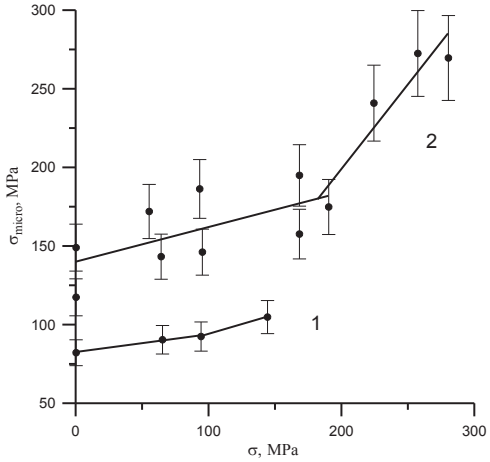

Figure 14. Variations of the microstresses operative in the Al matrix with macrostresses under loading:
Al – 5 wt.% C (1) and Al – 10 wt.% C (2).

Conclusions

It was shown that a highly disperse Al_4C_3 phase are formed during the hot pressing of Al-C nanocrystalline powder mixtures. The average crystallite size is 40 nm for the metal matrix and 30 nm for aluminum carbide.

The size of aluminum crystallites in the hot pressed samples was reduced by the presence of the Al_4C_3 nanoparticles formed during hot pressing and the formation of new interfaces in the material. This was also due to relatively rapid cooling from the temperature of hot pressing.

The crystallite size of the metal matrix decreases while that of the Al_4C_3 crystallites grows as the amount of aluminum carbide formed during synthesis increases.

Aluminum carbide formed in the process of hot pressing of Al–Al_4C_3 composites causes the yield stress $\sigma_{0.2}$ and the effective elastic modulus E_{ef} to increase. The higher is the amount of the reinforcement in the composite, the higher are $\sigma_{0.2}$ and E_{ef}.

The microstresses operative in the aluminum matrix are linearly dependent on applied macrostresses. The bend of the microstress-macrostress curve observed for $\sigma_{0.2}$ = 200 MPa is likely to be due to the attainment of the yield stress in the matrix.

References

1. W. S. Miller and F. J. Humphreys. Strengthening mechanisms in metal matrix composites in fundamental relation ships between microstructure and mechanical properties of metal-matrix composite. Warrendale.: TMS. 1990. P. 517.
2. L. Jiang, G. Wu, D. Sun, Q. Zhang, J. Chen. Microstructure and mechanical behavior of sub-micro particulate-reinforced Al matrix composites.// Journal of material science letters. 2002. №21. P. 609-611.
3. S.J. Lin, C.A. Lin, G.A. Wu, J.L. Horng. Sliding wear of Al_2O_{3p}/6061 Al composite. // Journal of material science. 1996. №31. P. 3481-3486
4. S.N. Kulkov and S.A. Vorozhtsov. Structure and mechanical behavior of Al-Al_4C_3 composites. Russian Physics Journal, 2011. Vol. 53. №11. pp. 1153-1157.
5. S.A. Vorozhtsov, S.P. Buyakova, S.N. Kulkov. Synthesis, Structure, and Phase Composition of Al-Al_4C_3 Nanostructured Materials. Russian Journal of Non-Ferrous Metals, 2012, Vol. 53, №5, pp. 420-424.
6. Lerner M.I. and Shamanskii V.V. Zh. Strukt. Khim., 2004, vol. 45, p. 112.
7. Komarov V.F., Sakovich G.V. and Potapov M.G., Nanostructured Thin Films and Nanodispersion Strengthened Coatings, Dordrecht: Kluger Academic, 2004.
8. A.A. Gromov, S.A. Vorozhtsov, V.F. Komarov, G.V. Sakovich, Yu. I. Pautova, M. Offermann. Ageing of nanodiamond powder: Physical characterization of the material. Materials Letters, 2013, Vol. 91, pp. 198-201.
9. Saltykov S.A., Stereometricheskaya metallografiya (Stereometric Metallography), Moscow: Metallurgiya, 1970.
10. Umanskii Ya.S., Skakov Yu.A., Ivanov A.N. and Rastorguev L.N. Kristallografiya, rentgenografiya i elektronnaya mikroskopiya (Crystallography, X-Ray Analysis, and Electron Microscopy), Moscow: Metallurgiya, 1982.
11. Sakovich G.V., Komarov V.F. and Petrov E.A., Sverkhtverd. Mater., 2002, no. 3, p. 3.
12. Besterci M., L'udovit Parilak, Metal. Mater. High Struct. Effic., 2004, vol. 146, no. 3, p. 195.
13. Streletskii A.N., Povstugar I.V., Borunova A.B., et al., Kolloidn. Zh., 2006, vol. 68, no. 4, p. 513.